


Diet-induced iron deficiency in rats impacts small intestinal calcium and phosphate absorption

Evans O. Asowata¹ | Oluwatobi Olusanya¹ | Kaoutar Abaakil¹ | Havovi Chichger² |
Surjit K. S. Srai³ | Robert J. Unwin⁴ | Joanne Marks¹ 

¹Department of Neuroscience, Physiology & Pharmacology, University College London, London, UK

²Biomedical Research Group, School of Life Sciences, Anglia Ruskin University, Cambridge, UK

³Institute of Structural and Molecular Biology, University College London, London, UK

⁴Department of Renal Medicine, University College London, London, UK

Correspondence

Joanne Marks, Department of Neuroscience Physiology & Pharmacology, University College London, Royal Free Campus, Rowland Hill Street, London NW3 2PF, UK.

Email: joanne.marks@ucl.ac.uk

Funding information

Nigerian Government; St Peter's Trust for Kidney, Bladder and Prostate Research

Abstract

Aims: Recent reports suggest that iron deficiency impacts both intestinal calcium and phosphate absorption, although the exact transport pathways and intestinal segment responsible have not been determined. Therefore, we aimed to systematically investigate the impact of iron deficiency on the cellular mechanisms of transcellular and paracellular calcium and phosphate transport in different regions of the rat small intestine.

Methods: Adult, male Sprague-Dawley rats were maintained on a control or iron-deficient diet for 2 weeks and changes in intestinal calcium and phosphate uptake were determined using the in situ intestinal loop technique. The circulating levels of the hormonal regulators of calcium and phosphate were determined by ELISA, while the expression of transcellular calcium and phosphate transporters, and intestinal claudins were determined using qPCR and western blotting.

Results: Diet-induced iron deficiency significantly increased calcium absorption in the duodenum but had no impact in the jejunum and ileum. In contrast, phosphate absorption was significantly inhibited in the duodenum and to a lesser extent the jejunum, but remained unchanged in the ileum. The changes in duodenal calcium and phosphate absorption in the iron-deficient animals were associated with increased claudin 2 and 3 mRNA and protein levels, while levels of parathyroid hormone, fibroblast growth factor-23 and 1,25-dihydroxy vitamin D₃ were unchanged.

Conclusion: We propose that iron deficiency alters calcium and phosphate transport in the duodenum. This occurs via changes to the paracellular pathway, whereby up-regulation of claudin 2 increases calcium absorption and upregulation of claudin 3 inhibits phosphate absorption.

KEYWORDS

calcium, claudin, intestine, iron deficiency, paracellular, phosphate

Evans O. Asowata and Oluwatobi Olusanya contributed equally to this work.

This is an open access article under the terms of the Creative Commons Attribution-NonCommercial-NoDerivs License, which permits use and distribution in any medium, provided the original work is properly cited, the use is non-commercial and no modifications or adaptations are made.

© 2021 The Authors. *Acta Physiologica* published by John Wiley & Sons Ltd on behalf of Scandinavian Physiological Society

1 | INTRODUCTION

The regulation of systemic iron homeostasis is essential for many biological processes, including the formation of the oxygen transport proteins, haemoglobin and myoglobin, and for the catalytic activity of many enzymes in the body. Systemic iron homeostasis is controlled by the peptide hormone hepcidin, which inhibits intestinal iron absorption in the duodenum via downregulation of the basolateral iron transporter ferroportin^{1,2} and the apical divalent metal transporter type 1 (DMT1).³ Recent evidence suggests that hepcidin also affects intestinal calcium transport^{4,5} and that iron deficiency may be a risk factor for the development of osteoporosis.⁶ Given that calcium and phosphate are key constituents of the bone mineral hydroxyapatite,⁷ it is possible that the absorption of these minerals in the small intestine might also be affected by iron deficiency. In keeping with this hypothesis, a limited number of studies have investigated the impact of iron deficiency on intestinal calcium and phosphate absorption. Phosphate absorption has been shown to increase⁸ in response to iron deficiency, while calcium absorption has been reported to both increase⁸ and decrease.⁹ The discrepancy in these findings may be caused by inconsistencies in the iron composition of the diets and the length of treatment, resulting in differences in the severity of iron deficiency. Importantly, no single study has been designed to determine systematically the impact of iron deficiency on the different transport pathways and cellular mechanisms involved in calcium and phosphate absorption in different regions of the small intestine.

Intestinal calcium and phosphate absorption occurs by both transcellular and paracellular mechanisms.^{10,11} The traditional model for transcellular calcium absorption is a three-step process involving calcium entry at the apical membrane via the transient receptor potential vullinoid 6 (TRPV6) channel,^{12,13} intracellular shuttling of calcium by calbindin D9k^{14,15} and basolateral membrane exit of calcium via the plasma membrane calcium ATPase 1b (PMCA-1b) and the sodium-calcium exchanger 1 (NCX-1).^{16,17} Less is known about the overall cellular processes responsible for transcellular phosphate transport, with the exception that it is critically dependent on the apical type II sodium-dependent phosphate co-transporter, NaPi-IIb.^{18,19} Transcellular calcium and phosphate absorption occurs in different regions of the small intestine: transcellular calcium transport occurring predominantly in the duodenum,²⁰ while the jejunum is the major site for transcellular phosphate absorption,^{21,22} at least in the rat. In contrast, absorption of calcium and phosphate via the paracellular pathway occurs in all three segments of the small intestine,^{20,23,24} and is likely to be the dominant route for absorption under normal or high levels of dietary calcium and phosphate intake.^{25,26}

Paracellular absorption of solutes and ions from the intestinal lumen into the circulation is influenced by the

composition and architectural organization of tight-junction complexes. Numerous integral membrane proteins and scaffold proteins combine to form tight junctions, but it is recognized that the claudin protein family plays a key role in the transport function of these complexes (reviewed in Ref.27). Claudins are known to form either epithelial barriers (sealing claudins) or paracellular channels (pore-forming claudins), and have been shown to have distinct regional profiles along the intestine.^{28,29} For example, claudin 3, a major sealing claudin that has recently been associated with paracellular phosphate absorption,³⁰ and has been demonstrated to be most highly expressed in the duodenum.²⁸ While the pore-forming claudins 2 and 12, which have a high conductance for calcium, are most abundantly expressed in the jejunum and ileum of rats.^{28,31} While it is widely recognized that 1,25-dihydroxy vitamin D₃ (1,25(OH)₂D₃) is responsible for regulating transepithelial calcium and phosphate absorption,^{32,33} evidence also suggests that it increases claudin 2 and 12 proteins levels in a vitamin D receptor (VDR)-dependent manner to enhance paracellular calcium absorption.³⁴ Intriguingly, the VDR agonist lithocholic acid (LCA) has recently been proposed to suppress claudin 3 levels, resulting in increased phosphate permeability in the small intestine.³⁰ Based on our growing understanding of the processes involved in calcium and phosphate absorption, and the potential that dietary iron deficiency alters the intestinal handling of these ions, the current study aimed to investigate the impact of iron deficiency on the cellular mechanisms of calcium and phosphate transport in different regions of the rat small intestine.

2 | RESULTS

2.1 | Diet-induced iron deficiency impacts intestinal phosphate and calcium absorption

Rats administered a diet containing 2-6 ppm of iron had the typical features of iron deficiency, including significantly decreased serum iron, plasma ferritin and hematocrit levels, and significantly increased UIBC (Table 1). The final weight of the animals after the 2-week dietary regime was similar in both groups (Table 1). Additionally, the animals exhibited the expected intestinal adaptation to dietary iron deficiency by significantly elevating DMT1 mRNA and protein levels in the duodenum (Figure 1).

Using the in situ intestinal loop technique and 10 mmol/L phosphate in the uptake buffer, diet-induced iron deficiency was shown to significantly inhibit total transepithelial phosphate absorption in the duodenum and jejunum (Figure 2A,B) but remained unchanged in the ileum (Figure 2C). However, this inhibition was more prominent in the duodenum (Figure 2A) compared with the jejunum (Figure 2B). Using

the same technique and with 100 mmol/L calcium in the uptake solution, total transepithelial calcium absorption was significantly higher in the duodenum of iron-deficient animals compared with control animals (Figure 2C) but remained unchanged in the jejunum (Figure 2D) and ileum (Figure 2E). The changes in duodenal phosphate and calcium absorption did not, however, significantly impact serum levels or urinary excretion of these two ions (Table 2).

TABLE 1 Effect of diet-induced iron deficiency on markers of iron status and animal weight

	Control	Iron deficient
Hematocrit (%)	42.38 ± 0.45	37.08 ± 0.75***
Serum iron (μmol/L)	36.50 ± 2.82	9.22 ± 1.15***
Serum UIBC (μg/dL)	357.20 ± 10.15	473.90 ± 8.13****
Plasma ferritin (ng/mL)	224.40 ± 59.46	41.45 ± 10.78*
Animal weight (g)	345.00 ± 13.41	333.60 ± 13.85

Note: Data are presented as mean ± SEM and analysed using an unpaired t-test. Haematocrit (*** P < .001, n = 12), serum iron (*** P < .001, n = 5-6), serum UIBC, (**** P < .0001, n = 8-9), plasma ferritin (* P < .05, n = 4-5) and weight of animals (n = 12).

2.2 | Effect of diet-induced iron deficiency on the levels of transcellular phosphate and calcium transporters

RT-PCR and western blotting experiments were performed to test if there were any changes in the mRNA and protein levels of the major transcellular phosphate and calcium transporters in response to diet-induced iron deficiency. In the duodenum, NaPi-IIb mRNA levels were significantly downregulated in iron-deficient animals (Figure 3A). However, the very low levels of duodenal NaPi-IIb mRNA (~10-fold lower than jejunum) (Figure 3A) and the lack of detectable NaPi-IIb protein in this segment (Figure 3B) raise the question of whether there is any physiological relevance of this downregulation for intestinal phosphate absorption. In contrast, NaPi-IIb mRNA (Figure 3A) and protein levels (Figure 3C) were unchanged in the jejunum in response to iron deficiency. As expected,^{21,32} NaPi-IIb mRNA levels were undetectable in the ileum (results not shown).

In keeping with previous studies, the segmental expression profile of TRPV6, Calbindin D9k and PMCA-1b showed a clear distinction, with the highest levels seen in the duodenum (Figure 4A-C).²⁰ While TRPV6 (Figure 4A) and NCX-1 (Figure 4D) expression was unaffected by iron

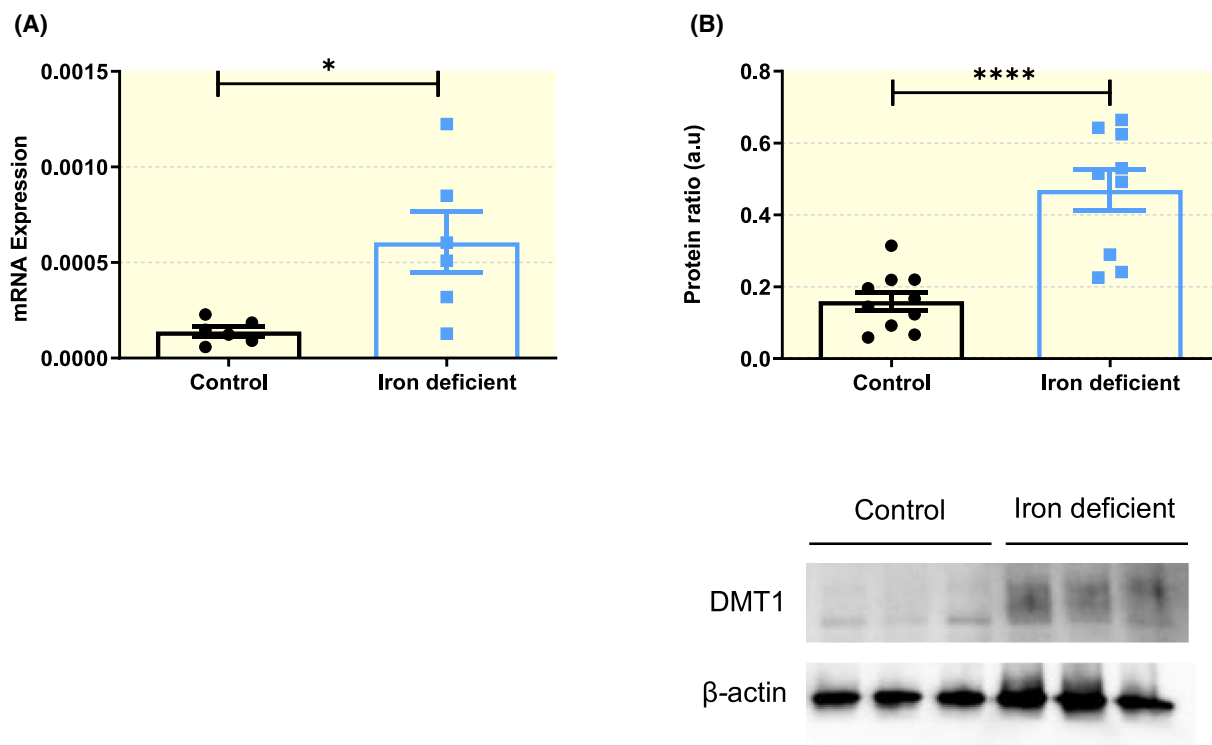


FIGURE 1 DMT1 mRNA and protein levels are increased in the duodenum by diet-induced iron deficiency. The effect of iron deficiency on duodenal DMT1 mRNA expression (A) was quantified using qPCR. Duplicate PCR reactions were performed for each sample and the mRNA expression of DMT1 given relative to β-actin mRNA levels. The effect of iron deficiency on duodenal DMT1 protein levels (B) was quantified by western blotting of BBM vesicles prepared from the intestine of control and iron-deficient animals. The bar graph shows the density of DMT1 relative to β-actin. An unpaired t-test was used to compare the differences between control and iron-deficient groups for both mRNA and protein levels (* P < .05, **** P < .0001, n = 6-10)

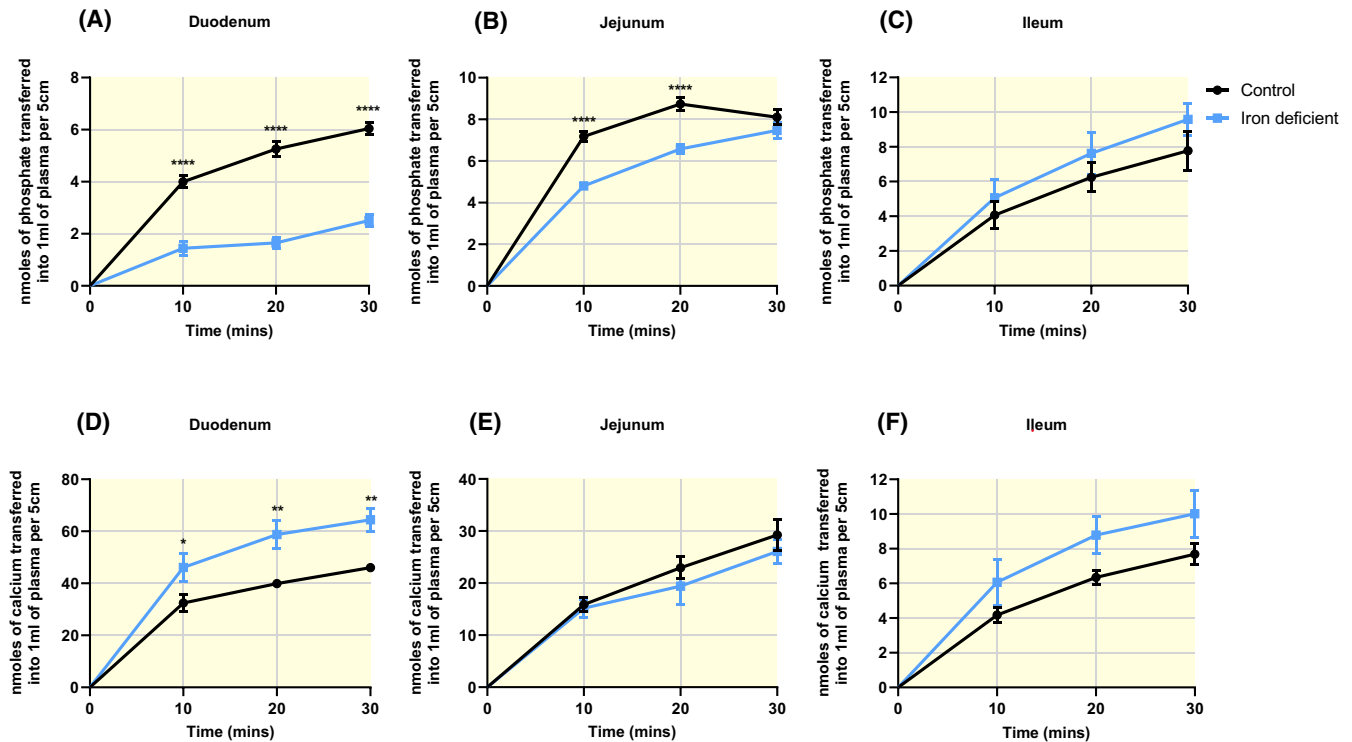


FIGURE 2 Diet-induced iron deficiency impacts intestinal phosphate and calcium absorption in vivo. Phosphate uptake in the duodenum (A) and jejunum (B) and ileum (C) was determined in vivo using buffer containing 10 mmol/L phosphate. Calcium uptake in the duodenum (D), jejunum (E) and ileum (F) was determined using a buffer containing 100 mmol/L calcium. Animals were maintained on a control (●) or iron-deficient diet (■) for 2 wk. A two-way ANOVA with Bonferroni multiple comparisons post-hoc test was used to compare differences between groups, * $P < .05$, ** $P < .01$, **** $P < .0001$ ($n = 4-8$)

deficiency, a significant decrease in duodenal calbindin D9k (Figure 4B) and jejunal PMCA-1b (Figure 4C) gene expression was observed. Because transcellular calcium transport occurs mainly in the duodenum, western blotting was used to investigate whether iron deficiency impacts the protein levels of the transcellular calcium transporters in this region. The results showed that duodenal calbindin D9k protein was significantly downregulated in response to iron deficiency (Figure 5B), while TRPV6, PMCA-1b and NCX-1 protein levels were unchanged (Figure 5A,C,D). The downregulation of calbindin D9k mRNA and protein levels as well as the unchanged levels of the other transcellular calcium transporters in the duodenum suggest that the transcellular calcium transport pathway does not contribute to the increase in duodenal calcium absorption observed in the iron-deficient animals.

2.3 | Diet-induced iron deficiency increases duodenal claudin 2 and 3 levels

Given that previous uptake studies using 10 mmol/L KH_2PO_4 ²² and 100 mmol/L CaCl_2 ²⁰ in the uptake buffer demonstrated that paracellular absorption is predominant under these conditions and that claudins are likely to be involved in the regulation of paracellular absorption, we used RT-PCR to

investigate the expression of intestinal claudins in response to iron deficiency. The results demonstrated that diet-induced iron deficiency significantly upregulated claudin 2 and 3 gene expression, but only in the duodenum (Figure 6A,B). In contrast, mRNA levels of the other highly expressed intestinal claudins 4, 7, 12 and 15, consistently reported in the small intestine of rodents,^{28,31,35} were unaffected by iron deficiency (Figure 6A-F). Western blotting also revealed that duodenal claudin 2 and 3 protein levels were significantly upregulated by diet-induced iron deficiency, confirming that increased mRNA levels translated to elevated claudin 2 and 3 protein in our model (Figures 7A and 8A).

Furthermore, while $1,25(\text{OH})_2\text{D}_3$ -VDR interaction plays a major role in regulating claudin 2 expression and paracellular calcium transport, VDR-dependent regulation of claudin 3 expression has been linked recently to changes in paracellular phosphate absorption in the small intestine.³⁰ To investigate whether the increases in duodenal claudin 2 and 3 mRNA and protein levels in iron deficiency were as a result of any changes in circulating levels of $1,25(\text{OH})_2\text{D}_3$ or its regulators, FGF-23 and PTH, the levels of these hormones were measured by ELISA. The results show that diet-induced iron deficiency had no effect on the levels of these hormones (Table 2), suggesting that they do not contribute to the altered calcium and phosphate absorption seen in iron deficiency.

TABLE 2 Effect of diet-induced iron deficiency on serum phosphate and calcium levels, urinary phosphate and calcium excretion and systemic regulators of these ions

	Control	Iron deficient
Serum iFGF-23 (pg/mL)	571.50 ± 66.06	461.50 ± 34.86
Serum cFGF-23 (pg/mL)	622.80 ± 84.35	543.70 ± 117.50
Plasma intact PTH (pg/mL)	87.71 ± 17.25	78.12 ± 11.09
Serum 1,25(OH) ₂ D ₃ (fmol/L)	150.70 ± 7.84	144.00 ± 7.18
Serum Phosphate (mmol/L)	3.48 ± 0.28	3.43 ± 0.11
Serum Calcium (mmol/L)	2.04 ± 0.02	2.09 ± 0.04
Urine Phosphate/Urine Creatinine	2.21 ± 0.15	2.09 ± 0.50
Urine Phosphate excretion (mmol/16 h)	0.198 ± 0.032	0.145 ± 0.007
Urine Calcium/Urine Creatinine	0.20 ± 0.02	0.22 ± 0.02
Urine Calcium excretion (mmol/16 h)	0.010 ± 0.001	0.008 ± 0.001

Note: Data are presented as mean ± SEM and analysed using an unpaired t-test. Serum phosphate (n = 6), serum calcium (n = 11-12), urinary phosphate-to-creatinine ratio and net urinary phosphate excretion (n = 4-5), urinary calcium-to-creatinine ratio and net urinary calcium excretion (n = 9-10), serum iFGF-23 (n = 7), serum cFGF-23 (n = 6), plasma intact PTH (n = 10-11) and serum 1,25(OH)₂D₃ (n = 6).

3 | DISCUSSION

Previous studies of the effect of iron deficiency on intestinal calcium and phosphate absorption have used models of long-term nutritional ferropenic anaemia and have established changes in absorption based on the measurement of dietary intake and subsequent faecal excretion.^{8,9} While these studies used Wistar rats and started the dietary treatment immediately after weaning, the treatment period (and therefore the severity of iron deficiency) appears to have differing effects on calcium handling, with 28 days of treatment decreasing and 40 days increasing apparent intestinal calcium absorption. Importantly, these studies describe the sum of absorption and secretion of these ions across the small intestine and colon, but do not provide information on which intestinal segments are involved in these processes. In the current study, we have used the in situ intestinal loop technique to measure transepithelial absorption of phosphate and calcium in specific intestinal segments in real time. Contrary to the suggestion that iron deficiency may increase intestinal phosphate absorption,⁸ using a more focused approach, our findings show that it significantly blunts phosphate absorption in the duodenum and to a lesser extent the jejunum. Interestingly, the impact

of iron deficiency on intestinal calcium handling is also localized to the duodenum, resulting in enhanced transepithelial calcium absorption in this segment. While our findings contrast with those published previously,^{8,9} it is likely, as highlighted above, that these discrepancies arise from differences in the timescale and severity of the iron deficiency. Our study used 6- to 7-week-old rats fed an iron-deficient diet for only 14 days as against the published studies that used 3-week-old rats treated for 28 or 40 days. In keeping with this suggestion is the finding by Campos *et al* that the critical period in the evolution of nutritional ferropenic anaemia is between 30 and 40 days, and it was at this later time point that they found increased intestinal calcium and phosphate absorption. This increase in absorption was associated with an increase in urinary excretion of these ions to maintain serum levels. In our study, the alteration we observed in duodenal absorption did not impact serum calcium or phosphate levels and did not change net urinary excretion, a measure that is commonly used to reflect net intestinal absorption.³⁶ Thus, the relatively mild dietary iron deficiency in our model is not comparable with severe longer-term nutritional anaemia. In addition, while mild iron deficiency causes localized changes in duodenal calcium and phosphate handling, the relatively short length and rapid transit time of this segment³⁷ may mean that these changes do not impact overall balance of these ions. Alternatively, given that the colon has the capacity for calcium¹¹ and phosphate^{22,24} transport, it is possible that this intestinal segment adapts to the altered duodenal absorption to maintain homeostasis. Importantly, although early studies showed that the colon has the capacity for both transcellular and paracellular calcium absorption and secretion,^{38,39} the role of the colon in phosphate handling and the mechanisms involved have not been studied in detail.

However, what our results do highlight is a potentially novel mechanism linking iron absorption to the regulation of paracellular calcium and phosphate absorption. In this context, it has been speculated previously that the formation of complexes between these ions reduces their bioavailability and therefore rates of absorption. For example, high oral calcium intake has been suggested to interfere with iron absorption; negatively charged molecules, such as phytate, the principle storage form of phosphorous in plants and seeds, appears to complex with calcium and iron to reduce their bioavailability, and phosphate binders commonly contain calcium or iron.^{40,41} However, these interactions occur within the intestinal lumen and have the potential to impact absorption throughout the small intestine. In contrast, in the present study, changes in absorption are confined to the duodenum, the region where iron transport occurs predominantly,⁴² suggesting a direct effect of altered iron absorption on the cellular mechanisms involved in phosphate and calcium absorption.

To investigate this aspect further, we focused on the impact of iron deficiency on the key proteins thought to be responsible

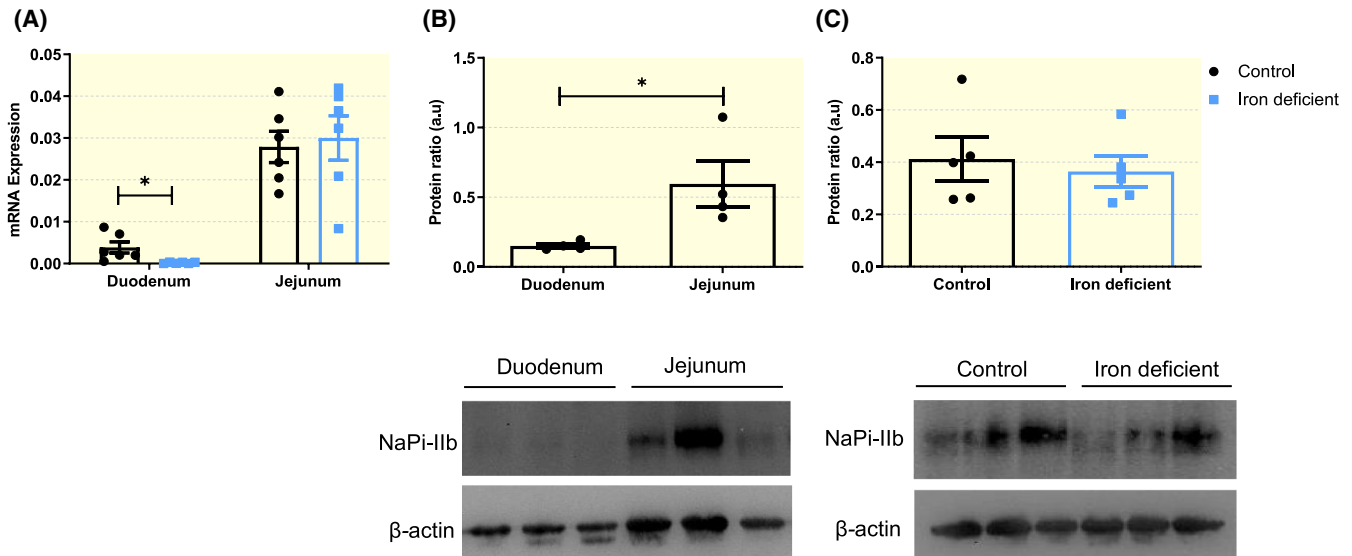


FIGURE 3 Effect of diet-induced iron deficiency on NaPi-IIb mRNA and protein. RT-PCR was used to determine the effect of iron deficiency on NaPi-IIb mRNA in the duodenum and jejunum (A). Duplicate PCR reactions were performed for each sample and the mRNA expression of NaPi-IIb is given as the ratio of NaPi-IIb to β -actin. An unpaired t-test was used to compare differences between groups ($*P < .05$, $n = 6$). The regional expression of NaPi-IIb protein in control rats (B) and the effect of iron deficiency on jejunal NaPi-IIb protein levels (C) were quantified by western blotting of BBM vesicles prepared from the intestine of control and iron-deficient animals. The bar graphs show the density of NaPi-IIb relative to β -actin, with results compared using an unpaired t-test ($*P < .05$, $n = 4-5$)

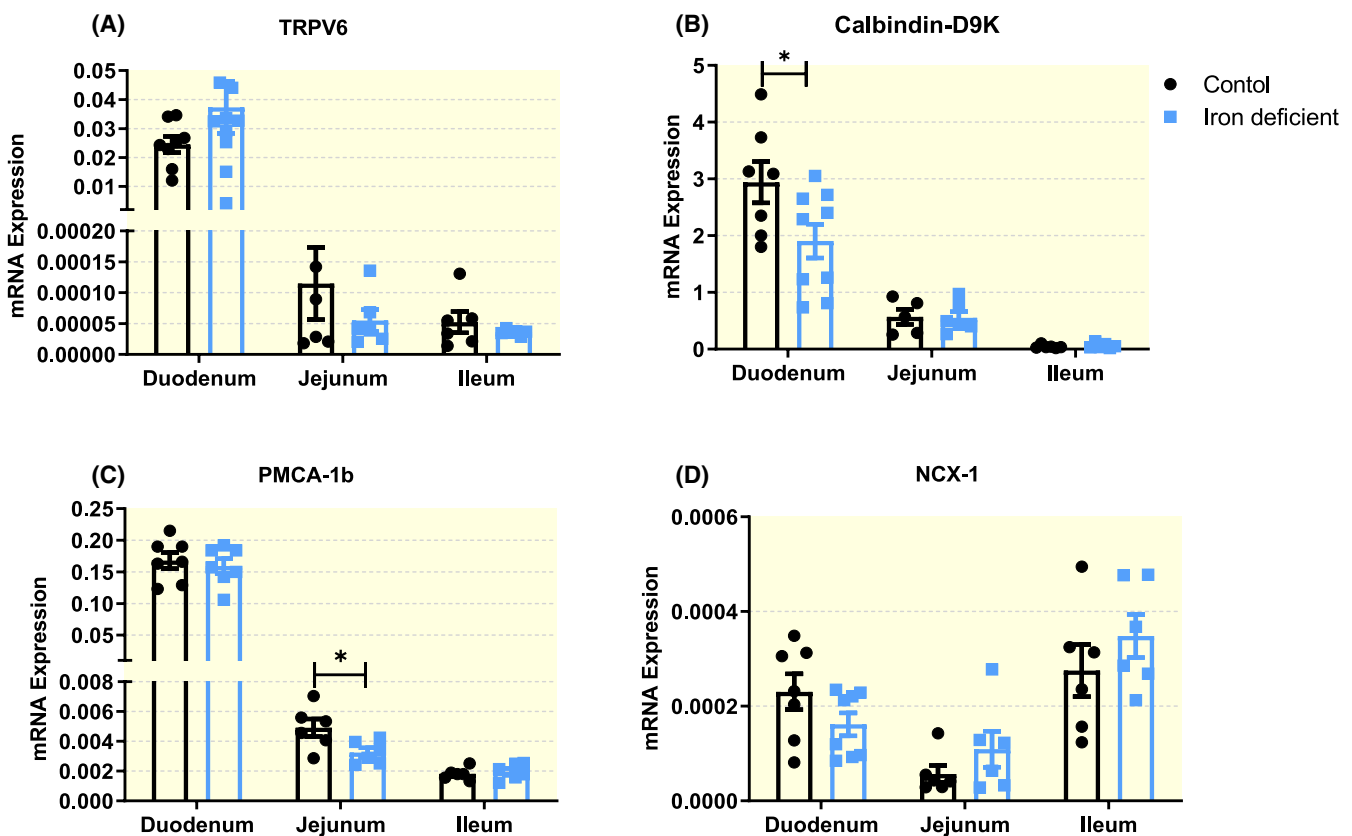


FIGURE 4 Effect of diet-induced iron deficiency on the mRNA expression of transcellular calcium transporters in the small intestine. RT-PCR was used to determine the effect of iron deficiency on the mRNA expression of TRPV6 (A), calbindin D9K (B), PMCA-1b (C) and NCX-1 (D) in the duodenum, jejunum and ileum. Duplicate PCR reactions were performed for each sample and the mRNA expression of each transporter is given as its ratio to β -actin. An unpaired t-test was used to compare differences between groups ($*P < .05$, $n = 5-10$)

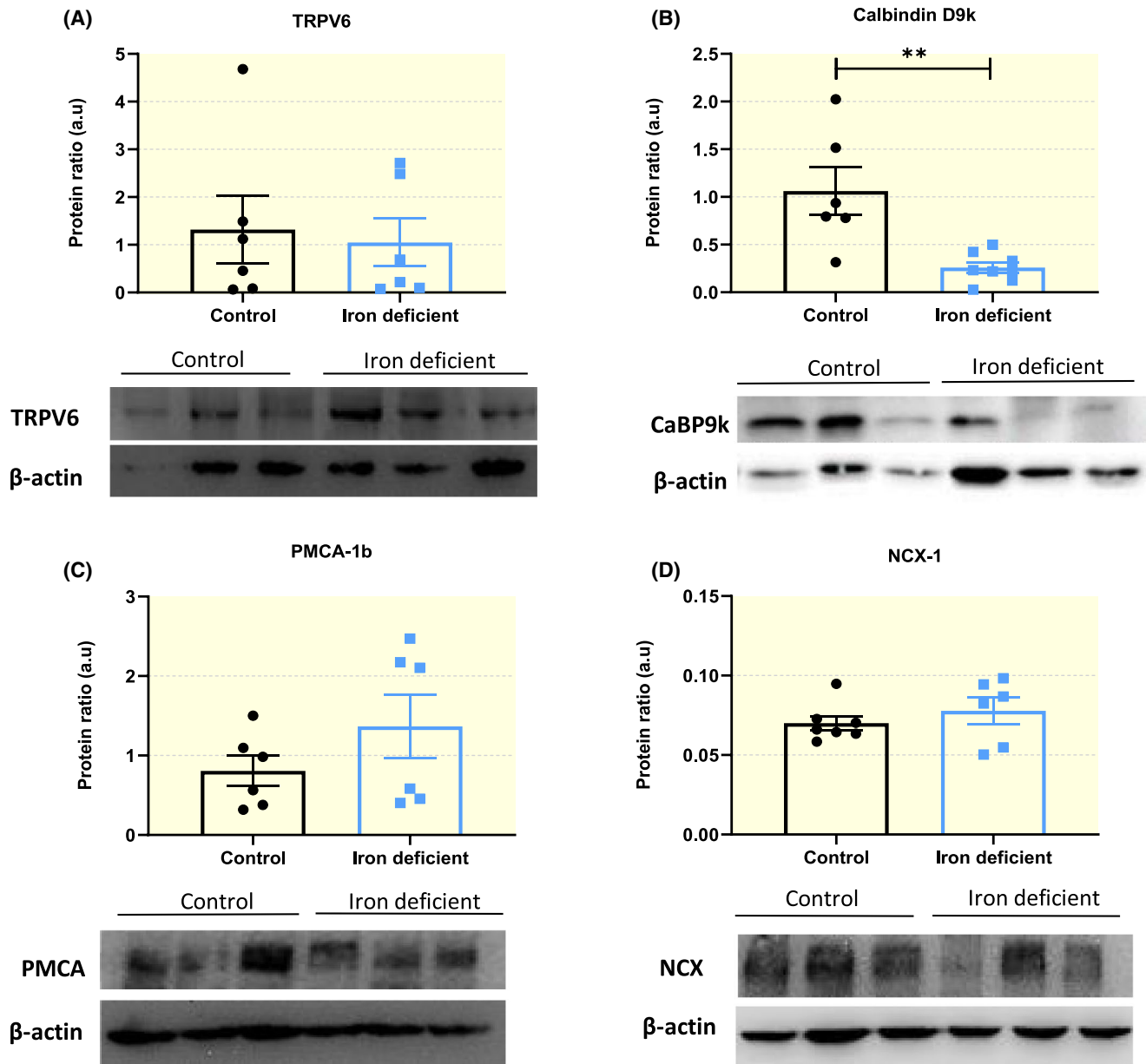


FIGURE 5 Effect of diet-induced iron deficiency on the protein levels of transcellular calcium transporters in the small intestine. Representative western blot image and quantification of TRPV6 (A), calbindin D9K (B), PMCA-1b (C) and NCX-1 (D) protein level in the duodenum. The abundance of protein is given as the ratio of protein of interest band density to β -actin, expressed in arbitrary units (a.u). An unpaired t-test was used to compare differences between groups (** $P < .01$, $n = 6-8$)

for transcellular phosphate and calcium handling in different regions of the small intestine. This pathway has been extensively studied for both ions and undergoes significant regulation, making it a plausible candidate for the observed changes in intestinal transport. NaPi-IIb is widely considered to be the rate-limiting step for transcellular phosphate absorption and the results of the current study, together with previous findings using gene chip analysis and quantitative PCR,^{43,44} show that in response to diet-induced iron deficiency NaPi-IIb gene levels are downregulated in the rat duodenum. However, our findings of very low expression of NaPi-IIb mRNA and undetectable protein levels in this intestinal segment provide evidence that

the inhibition of duodenal phosphate absorption by iron deficiency is unlikely to be dependent on NaPi-IIb-mediated transcellular transport. Similarly, if alterations in the key cellular components described for active transcellular calcium absorption, an increase in one or more of these proteins would be expected.⁴⁰ We show that the mRNA and protein levels of the components involved in apical or basolateral calcium flux are unchanged and that there is a significant reduction in calbindin D9k levels. These findings make it unlikely that this pathway is responsible for the increase in duodenal calcium absorption seen in iron-deficient rats.

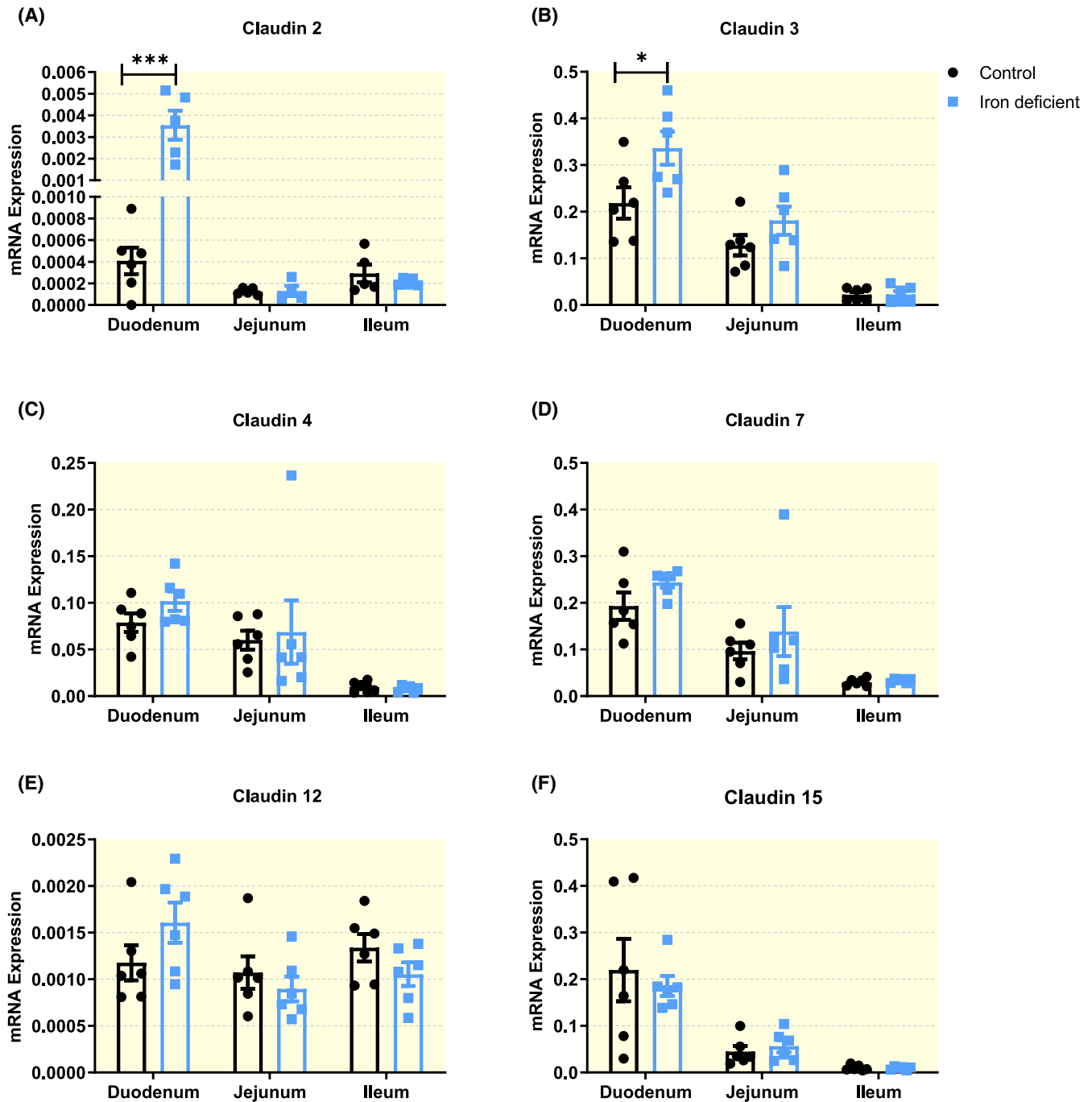


FIGURE 6 Effect of diet-induced iron deficiency on the mRNA expression of intestinal claudins. RT-PCR was used to determine the effect of iron deficiency on the mRNA expression of claudin 2 (A), claudin 3 (B), claudin 4 (C), claudin 7 (D), claudin 8 (E), claudin 12 (F) and claudin 15 (G) in the duodenum, jejunum and ileum. Duplicate PCR reactions were performed for each sample and the mRNA expression of each claudin is given as its ratio to β -actin. An unpaired t-test was used to compare differences between groups (* $P < .05$, *** $P < .001$, $n = 5-10$)

Instead, our results provide evidence for the involvement of the paracellular pathway in the altered duodenal calcium and phosphate handling. We specifically selected an uptake buffer containing these ions in the millimolar range to allow us to investigate the impact of iron deficiency on the paracellular component of absorption, since the transcellular pathway for these ions is expected to be saturated at these concentrations.⁴⁵⁻⁴⁷ Our reasoning being

that paracellular absorption is likely to be the dominant route under normal or high levels of dietary calcium and phosphate intake.^{25,26} Based on these assumptions and the lack of changes in the transcellular components of absorption, we investigated whether the specific claudins thought to be involved in paracellular calcium and phosphate absorption were altered in iron-deficient rats. Our results show that iron deficiency elevated levels of claudin 2 and

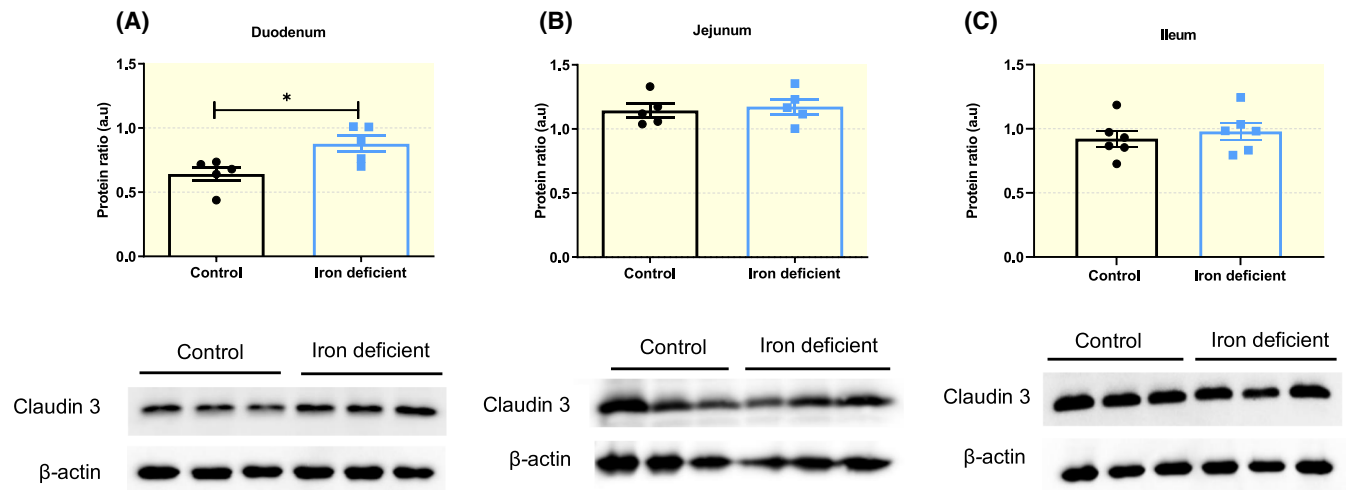


FIGURE 7 Diet-induced iron deficiency increases claudin 3 protein levels in the duodenum. Representative western blot image and quantification of claudin 3 protein levels in the duodenum (A), jejunum (B) and ileum (C) of control and iron-deficient animals. The abundance of claudin 3 protein is given as the ratio of claudin 3 band density to β -actin, expressed in arbitrary units (a.u). An unpaired t-test was used to compare results between groups (* $P < .05$, $n = 5-6$)

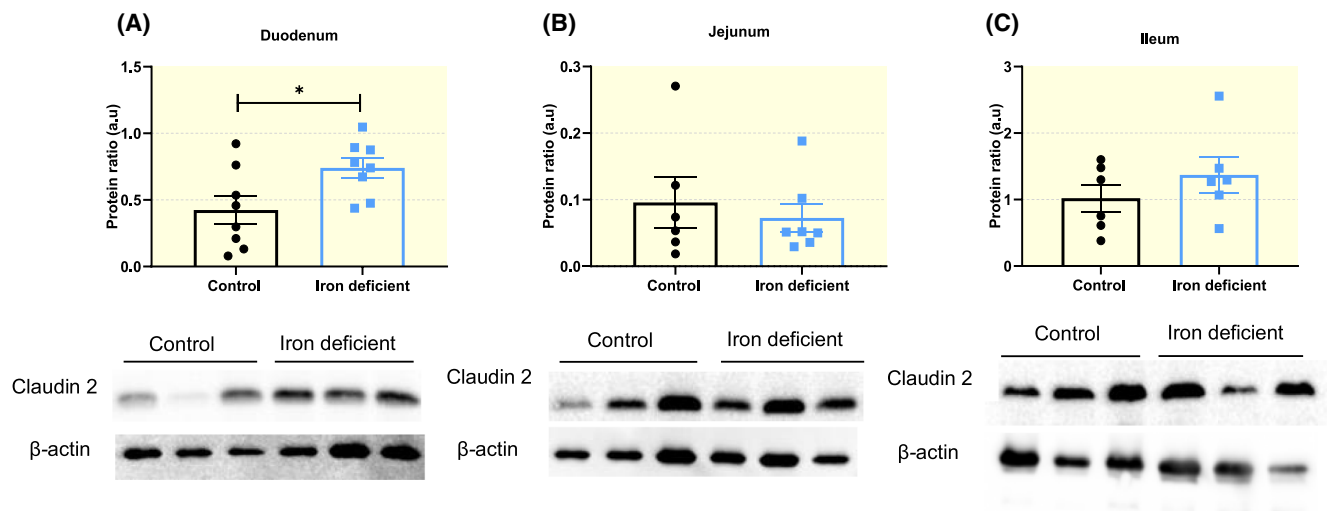


FIGURE 8 Diet-induced iron deficiency increases claudin 2 protein levels in the duodenum. Representative western blot image and quantification of claudin 2 protein levels in the duodenum (A), jejunum (B) and ileum (C) of control and iron-deficient animals. The abundance of claudin 2 protein is given as the ratio of claudin 2 band density to β -actin, expressed in arbitrary units (a.u). An unpaired t-test was used to compare results between groups (* $P < .05$, $n = 6-8$)

claudin 3 mRNA and protein, and that these changes were confined to the duodenum, the region where we demonstrated altered rates of absorption. Importantly, there is growing evidence linking claudin 2 with paracellular calcium transport in both the kidney and small intestine (reviewed in Ref.37,48). This protein has negatively charged amino acids in the extracellular domains that project into the paracellular space to form a tight junction pore, which confers charge selectivity.^{49,50} Upregulated claudin 2 expression and high luminal calcium levels should favour conductance of the cation across the paracellular space. This has been confirmed by Fujita *et al* who demonstrated that

overexpression or siRNA knockdown of claudin 2 in the intestinal epithelial caco-2 cell line increased and decreased calcium permeability respectively. In addition, treatment of these cells with $1,25(\text{OH})_2\text{D}_3$ increased claudin 2 mRNA and protein levels and subsequent knockdown of claudin 2 resulted in a significant decrease in $1,25(\text{OH})_2\text{D}_3$ -induced calcium permeability.³⁴ Therefore, based on these earlier findings, the upregulation of claudin 2 mRNA and protein levels demonstrated in the current study is the most likely contributor to the increase in duodenal calcium absorption seen in response to iron deficiency. However, it should be noted that while a recent study by Curry *et al* established

that claudin 2 knockout mice have a decrease in passive calcium permeability, this adaptation is confined to the colon, where under normal physiological conditions the protein is likely to mediate calcium secretion.⁵¹ Whether differences in the regional profile of claudin 2 in rats versus mice, combined with the local environment in which the protein is maximally expressed, impact the absorptive or secretory function of this protein requires further investigation. In contrast to our understanding of the role of claudins in paracellular calcium absorption, until recently little has been known on whether claudin(s) are also involved in the regulation of paracellular phosphate transport. However, a recent study has shown that phosphate, but not calcium, absorption in the jejunum and ileum of claudin 3 knockout mice is significantly increased, suggesting that this sealing claudin plays a role in paracellular phosphate absorption.³⁰ In keeping with this suggestion, our study shows that the substantial inhibition of phosphate absorption in the duodenum is associated with upregulation of claudin 3 mRNA and protein levels, while in the jejunum, where diet-induced iron deficiency had only a minor impact on phosphate absorption, claudin 3 remained unchanged.

Since the levels of claudin 2 and 3 have been reported to be sensitive to circulating levels of $1,25(\text{OH})_2\text{D}_3$ ^{34,52} and activation of VDR by lithocholic acid impacts paracellular phosphate absorption via a reduction in claudin 3 levels,³⁰ we investigated whether changes in $1,25(\text{OH})_2\text{D}_3$ were responsible for the altered calcium and phosphate absorption seen in iron deficiency. The finding that iron deficiency had no effect on $1,25(\text{OH})_2\text{D}_3$ or its regulators, PTH and FGF-23, suggests that upregulation of duodenal claudin 2 and 3 observed in the current study was not caused by changes in the levels of these hormones. Instead, we speculate that changes in claudin 2 and 3 in iron deficiency may be directly related to a decrease in intracellular pH in duodenal enterocytes as a result of the increased iron absorption seen in this segment.⁵³

In summary, the present study investigated the effect of diet-induced iron deficiency on calcium and phosphate absorption in the small intestine of male, adult rats. Because the consumption of high levels of calcium and phosphate from dairy products and processed food is increasingly common, we used uptake buffers containing these ions at concentrations intended to mimic levels normally present in the small intestine.^{22,54} Our findings demonstrate that short-term diet-induced iron deficiency increases calcium absorption and inhibits phosphate absorption in the rat duodenum by mechanisms that involve changes in the paracellular pathway. We propose that in iron-deficient rats, upregulation of duodenal claudin 2, a cation-selective pore-forming protein, is responsible for the increase in calcium absorption, while increased levels of duodenal claudin 3, a sealing protein, result in the inhibition of phosphate absorption.

4 | MATERIALS AND METHODS

4.1 | Animals and diets

Male 5- to 6-week-old Sprague-Dawley rats (180–200 g) were purchased from Charles River Laboratories (Harlow, UK). Rats were either fed a control iron diet (TD. 80394) containing 48 ppm added iron or an iron-deficient diet (TD. 80396) containing approximately 2–6 ppm added iron for 2 weeks. Other than the iron content, both diets had the same composition, and contained 0.6% phosphate. All diets were purchased from Harlan Laboratories, Inc Madison, WI, USA. A maximum of three rats were housed in the same cage on a 12-h light/dark cycle, with free access to food and water. For urine collection following the 2-week period of diet administration, animals were individually housed in metabolic cages for 16 hours. All procedures were approved by University College London (Royal Free Campus) Comparative Biology Unit Animal Welfare and Ethical Review Body (AWERB) committee and conducted in accordance with the UK legislation (Animal Scientific Procedures act, 1986, Amendment regulations 2012).

4.2 | In situ intestinal phosphate and calcium uptake experiments

In situ intestinal loop experiments were carried out as described previously.⁵⁵ In brief, animals were anaesthetized by an intraperitoneal injection of 45 mg/kg pentobarbitone sodium (Pentobarbitone; Animal care Ltd, UK) and the depth of anaesthesia was confirmed and monitored by checking the reflexes (corneal, tail pinch and pedal withdrawal). Phosphate or calcium uptake solution (500 μL) was instilled into a 5-cm-long segment of cannulated duodenum (approximately 2 cm from the pylorus), jejunum (approximately 5 cm from the ligament of Trietz) or ileum (approximately 5 cm proximal to the cecum). For phosphate uptake experiments, uptake solution containing 16 mmol/L sodium-HEPES, 140 mmol/L NaCl, 3.5 mmol/L KCl and 10 mmol/L KH_2PO_4 (pH 7.4) and 0.37 MBq ^{33}P (PerkinElmer, Bucks, UK) was instilled into the lumen of the cannulated intestinal segment and immediately tied off. Calcium uptakes used a similar uptake solution, but with the phosphate replaced with 100 mmol/L CaCl_2 and 0.37 MBq ^{45}Ca (PerkinElmer, Bucks, UK). Blood (~500 μL) was collected from the cannulated femoral artery at 10, 20 and 30 minutes after instilling the uptake solution. After 30 minutes, the intestinal segment was removed, blotted and the length was measured and recorded. The remaining intestinal segments were removed for use in western blotting or qPCR and the animal exsanguinated via cardiac puncture, with death ensured by incising the heart. The amount of phosphate or calcium transferred from the intestinal segment into 1 mL of plasma was calculated using data obtained from

scintillation counting (Tri-Carb 2900TR; Perkin Elmer) of plasma and the initial uptake solution.

4.3 | Blood and urine biochemistry

Blood samples were collected at the end of the experiment by cardiac puncture and haematocrit measured using a micro-haematocrit reader. Blood was centrifuged at 1500 g for 15 minutes at 4°C to obtain serum or plasma, and serum samples were sent to the Chemical Pathology Department in the Royal Free Hospital for the measurement of serum iron. All other assays were carried out following manufacturer's instructions. Serum unsaturated iron-binding capacity (UIBC) was measured using a commercially available kit (Pointe Scientific Inc, Canton, MI, USA) and plasma ferritin was measured using a rat-specific ELISA kit (Abcam, Cambridge, UK). Serum and urine phosphate and calcium levels were measured using colorimetric phosphate (Biovision Inc, CA, USA) or calcium (GeneTex, CA, USA) assay kits, and urinary creatinine levels determined using the Jaffe method.⁵⁶ Serum intact fibroblast growth factor-23 (iFGF-23) (Kainos Laboratories Inc, Tokyo, Japan), C-terminal FGF-23 (cFGF-23) (Immutopics, Inc, San Clemente, CA, USA), 1,25(OH)₂D₃ (LSBio Inc, Seattle, WA, USA) and plasma intact parathyroid hormone (PTH) (Immutopics, Inc, San Clemente, CA, USA) were also measured by ELISA.

4.4 | Brush border membrane vesicle preparation

After opening the duodenum, jejunum and ileum longitudinally, mucosa was scraped off using glass slides. The mucosa was then snap frozen and stored at −80°C until use. Intestinal brush border membrane (BBM) vesicles were subsequently prepared using the MgCl₂ precipitation method as described previously.³² The protein concentration of BBM vesicles isolated from all three intestinal segment was determined using a Bradford assay.⁵⁷ To validate the purity of the BBM vesicles, alkaline phosphatase levels in the initial homogenate and the BBM vesicles were measured using the method of Forstner et al.⁵⁸ The BBM vesicles were approximately 10-fold enriched. All the steps in the isolation of the BBM vesicles were carried out at 4°C.

4.5 | Western blotting

Intestinal BBM vesicles or homogenate (20–50 µg protein) was mixed with laemmli sample buffer and separated on either a 10% or a 16% SDS-polyacrylamide gel (depending on the

molecular weight of the protein of interest). The proteins were transferred on to a polyvinylidene difluoride (PVDF) membrane by electroblotting at 15 V for 75 minutes (for proteins with a size above 30 kDa) or 10 V for 20 minutes (for proteins with a size below 30 kDa). The PVDF membranes were then blocked with 6% fat-free milk in PBS containing 0.1% Tween 20 (PBS-T), for 1 hour at room temperature, after which they were incubated with NaPi-IIb, DMT1, TRPV6, Calbindin D9k, PMCA-1b, NCX-1, claudin 2 or 3 antibodies (See Table 1 for supplier information and dilutions) for 16 hours at 4°C. The membranes were then washed with PBS-T four times (1× for 15 minutes and 3× for 5 minutes each) and then incubated with an anti-mouse (1:5000 dilution, Sigma Ltd, Amersham, UK) or anti-rabbit antibody conjugated to horseradish peroxidase (1:2000 dilution, GE Healthcare, Buckinghamshire, UK) for 1 hour at room temperature. The membranes were washed with PBS-T as described above and the bound antibodies were visualized by enhanced chemiluminescence using a Flour-S Multi-Imager System (Biorad, Hemmel Hempstead, UK) or a c600 azure imager (Azure Biosystems, Inc, San Francisco, CA, USA), with an acquisition time of 3 minutes. Owing to sample number (n = 5–6) for each group, quantitative comparison between samples run on two gels was required. These gels were processed in parallel and each was loaded with an equal number of control and iron-deficient samples. The membranes were stripped of the antibodies using Restore™ western blot stripping buffer (Thermo Scientific, Hemmel Hempstead, UK) and non-specific protein binding was blocked with PBS-T containing 6% fat-free milk as described above. The membranes were then incubated with a mouse monoclonal antibody raised against β-actin (Table S1) for 1 hour at room temperature. The membranes were washed and re-incubated with an anti-mouse secondary antibody (1:5000 dilution, Sigma Ltd, Amersham, UK) for 1 hour at room temperature and then visualized. Densitometric analysis was performed using the Flour-S Multi-Imager software or imageJ and the ratio of the protein of interest to β-actin band density was calculated for each sample and presented as arbitrary units (a.u). The molecular weight of each protein was calculated using the AzureSpot analysis software.

4.6 | Quantitative PCR

Total RNA was isolated from the scraped duodenal, jejunal and ileal mucosa using TRIzol™ reagent according to manufacturer's instructions (Life Technologies, Paisley, UK). One µg RNA was treated with deoxyribonuclease I (Life Technologies, Paisley, UK) and complementary DNA (cDNA) was synthesized by reverse transcription using a cDNA synthesis kit (PCR Biosystems Ltd, London, UK), following manufacturer's instructions. The expression levels of the genes of interest were analysed by real-time quantitative PCR (RT-PCR) using qPCRBIO SyGreen kit

(PCR Biosystems Ltd, London, UK) and rat-specific primers (Table S2) purchased from Qiagen (UK). Using a Light Cycler 96 instrument (Roche Diagnostics, East Sussex, UK), cycling conditions were as follows: pre-incubation at 95°C for 10 minutes, three-step amplification consisting of: 95°C for 10 seconds, 60°C for 10 seconds and 72°C for 10 seconds. A total of 35 or 45 cycles depending on the level of gene expression were carried out followed by a melting step consisting of 95°C for 10 seconds, 60°C for 60 seconds and 97°C for 1 second. The final condition of the melting stage was continuous with five readings recorded per unit temperature. The data were analysed using the Light Cycler 96 analysis software and the relative quantification (Rel Quant) of the mRNA for each gene of interest relative to β -actin was determined.

4.7 | Statistical analysis

Data are presented as mean \pm standard error of mean (SEM). Statistical analysis was performed using either an unpaired Student's *t* test, one-way ANOVA or a two-way ANOVA, with Tukey multiple comparisons post-hoc test where relevant. All analyses were performed using GraphPad Prism 8 software, and statistical significance depicted as **P* < .05, ***P* < .01, ****P* < .001 or *****P* < .0001.

ACKNOWLEDGEMENTS

This research was supported by a PhD scholarship awarded to EO Asowata by the Nigerian Government, funding from the St Peter's Trust for Kidney, Bladder and Prostate Research and personal PhD funding by O Olusanya.

CONFLICT OF INTEREST

The authors declare that they have no competing financial interests. Robert Unwin is Professor Emeritus of Nephrology at UCL and currently working in Early Clinical Development, Early CVRM (Cardiovascular, Renal and Metabolism), R&D BioPharmaceuticals, AstraZeneca, Cambridge, UK and Gothenburg, Sweden. Evans O. Asowata currently works as a postdoctoral scientist in Early CVRM, R&D BioPharmaceuticals, AstraZeneca, Cambridge, UK.

AUTHOR CONTRIBUTIONS

EO Asowata, SKS Srai, RJ Unwin, H Chichger and J Marks designed the research; EO Asowata, O Olusanya, K. Abaakil and J Marks performed the research and analysed the data. EO Asowata, O Olusanya and J Marks wrote the study. All authors approved the final version for publication.

DATA AVAILABILITY STATEMENT

The data that support the findings of this study are available from the corresponding author upon reasonable request.

ORCID

Joanne Marks  <https://orcid.org/0000-0002-2677-2477>

REFERENCES

1. Nemeth E, Tuttle MS, Powelson J, et al. Heparin regulates cellular iron efflux by binding to ferroportin and inducing its internalization. *Science* (80-). 2004;306(5704):2090-2093.
2. De Domenico I, Ward DM, Langelier C, et al. The molecular mechanism of hepcidin-mediated ferroportin down-regulation. *Mol Biol Cell*. 2007;18(7):2569-2578.
3. Brasselagnel C, Karim Z, Letteron P, Bekri S, Bado A, Beaumont C. Intestinal DMT1 cotransporter is down-regulated by hepcidin via proteasome internalization and degradation. *Gastroenterology*. 2011;140(4):1261-1271.
4. Kraidith K, Svasti S, Teerapornpuntakit J, et al. Heparin and 1,25(OH)₂D₃ effectively restore Ca²⁺ transport in β -thalassemic mice: Reciprocal phenomenon of Fe²⁺ and Ca²⁺ absorption. *Am J Physiol - Endocrinol Metab*. 2016;311(1):E214-E223.
5. Charoenphandhu N, Kraidith K, Lertsuwan K, et al. Na⁺/H⁺ exchanger 3 inhibitor diminishes hepcidin-enhanced duodenal calcium transport in hemizygous β -globin knockout thalassemic mice. *Mol Cell Biochem*. 2017;427(1-2):201-208.
6. Toxqui L, Vaquero MP. Chronic iron deficiency as an emerging risk factor for osteoporosis: a hypothesis. *Nutrients*. 2015;7(4):2324-2344.
7. Bonjour JP. Calcium and phosphate: a duet of ions playing for bone health. *J Am Coll Nutr*. 2011;30(5 Suppl 1):438S-448S.
8. Campos MS, Barrionuevo M, Alf  rez MJ, et al. Interactions among iron, calcium, phosphorus and magnesium in the nutritionally iron-deficient rat. *Exp Physiol*. 1998;83(6):771-781.
9. Katsumata S, Katsumata-Tsuboi R, Uehara M, Suzuki K. Severe iron deficiency decreases both bone formation and bone resorption in rats. *J Nutr*. 2009;139(2):238-243.
10. Sabbagh Y, Giral H, Caldas Y, Levi M, Schiavi SC. Intestinal phosphate transport. *Adv Chronic Kidney Dis*. 2011;18(2):85-90.
11. Christakos S, Dhawan P, Porta A, Mady LJ, Seth T. Vitamin D and intestinal calcium absorption. *Mol Cell Endocrinol*. 2011;347(1-2):25-29.
12. Bin PJ, Chen XZ, Berger UV, et al. Molecular cloning and characterization of a channel-like transporter mediating intestinal calcium absorption. *J Biol Chem*. 1999;274(32):22739-22746.
13. Peng J-B, Suzuki Y, Gyimesi G, Hediger MA. TRPV5 and TRPV6 calcium-selective channels. In: Kozak JA, Putney JWJ, eds. *Calcium Entry Channels in Non-Excitable Cells*. Florida, CA: CRC Press/Taylor & Francis; 2018:241-274.
14. Hong EJ, Jeung EB. Biological significance of calbindin-D9k within duodenal epithelium. *Int J Mol Sci*. 2013;14(12):23330-23340.
15. Bronner F. Mechanisms of intestinal calcium absorption. *J Cell Biochem*. 2003;88(2):387-393.
16. Hildmann B, Schmidt A, Murer H. Ca⁺⁺-transport across basal-lateral plasma membranes from rat small intestinal epithelial cells. *J Membr Biol*. 1982;65(1-2):55-62.
17. Hoenderop GJ, Nilius B, Bindels RJM. Calcium absorption across epithelia. *Physiol Rev*. 2005;85(1):373-422.
18. Sabbagh Y, O'Brien SP, Song W, et al. Intestinal Npt2b plays a major role in phosphate absorption and homeostasis. *J Am Soc Nephrol*. 2009;20(11):2348-2358.

19. Hernando N, Myakala K, Simona F, et al. Intestinal depletion of NaPi-IIb/Slc34a2 in mice: renal and hormonal adaptation. *J Bone Miner Res.* 2015;30(10):1925-1937.
20. Pansu D, Bellaton C, Roche C, Bronner F. Duodenal and ileal calcium absorption in the rat and effects of vitamin D. *Am J Physiol - Gastrointest Liver Physiol.* 1983;7(6):G695-G700.
21. Giral H, Caldas Y, Sutherland E, et al. Regulation of rat intestinal Na-dependent phosphate transporters by dietary phosphate. *Am J Physiol Renal Physiol.* 2009;297(5):F1466-F1475.
22. Marks J, Lee GJ, Nadaraja SP, Debnam ES, Unwin RJ. Experimental and regional variations in Na⁺-dependent and Na⁺-independent phosphate transport along the rat small intestine and colon. *Physiol Rep.* 2015;3(1):e12281.
23. Bronner F, Pansu D, Stein WD. An analysis of intestinal calcium transport across the rat intestine. *Am J Physiol Gastrointest Liver Physiol.* 1986;250(5):G561-G569.
24. Knöpfel T, Himmerkus N, Günzel D, Bleich M, Hernando N, Wagner CA. Paracellular transport of phosphate along the intestine. *Am J Physiol - Gastrointest Liver Physiol.* 2019;317(2):G233-G241.
25. Khanal RC, Nemere I. Regulation of intestinal calcium transport. *Annu Rev Nutr.* 2008;28(1):179-196.
26. Marks J. The role of SLC34A2 in intestinal phosphate absorption and phosphate homeostasis. *Pflügers Arch.* 2018;471(1):165-173.
27. Van Itallie CM, Anderson JM. Architecture of tight junctions and principles of molecular composition. *Semin Cell Dev Biol.* 2014;36:157-165.
28. Markov AG, Veshnyakova A, Fromm M, Amasheh M, Amasheh S. Segmental expression of claudin proteins correlates with tight junction barrier properties in rat intestine. *J Comp Physiol B Biochem Syst Environ Physiol.* 2010;180(4):591-598.
29. Amasheh S, Fromm M, Günzel D. Claudins of intestine and nephron - a correlation of molecular tight junction structure and barrier function. *Acta Physiol.* 2011;201(1):133-140.
30. Hashimoto N, Matsui I, Ishizuka S, et al. Lithocholic acid increases intestinal phosphate and calcium absorption in a vitamin D receptor dependent but transcellular pathway independent manner. *Kidney Int.* 2020;97(6):1164-1180.
31. Lu Z, Ding L, Lu Q, Chen Y-H. Claudins in intestines. *Tissue Barriers.* 2013;1(3):e24978.
32. Marks J, Srai SK, Biber J, Murer H, Unwin RJ, Debnam ES. Intestinal phosphate absorption and the effect of vitamin D: a comparison of rats with mice. *Exp Physiol.* 2006;91(3):531-537.
33. Song Y, Peng X, Porta A, et al. Calcium transporter 1 and epithelial calcium channel messenger ribonucleic acid are differentially regulated by 1,25 dihydroxyvitamin D₃ in the intestine and kidney of mice. *Endocrinology.* 2003;144(9):3885-3894.
34. Fujita H, Sugimoto K, Inatomi S, et al. Tight junction proteins claudin-2 and -12 are critical for vitamin D-dependent Ca²⁺ absorption between enterocytes. *Mol Biol Cell.* 2008;19(5):1912-1921.
35. Rahner C, Mitic LL, Anderson JM. Heterogeneity in expression and subcellular localization of claudins 2, 3, 4, and 5 in the rat liver, pancreas, and gut. *Gastroenterology.* 2001;120(2):411-422.
36. Cupisti A, Gallieni M. Urinary phosphorus excretion: not what we have believed it to be? *Clin J Am Soc Nephrol.* 2018;13(7):973-974.
37. Alexander RT, Rievaj J, Dimke H. Paracellular calcium transport across renal and intestinal epithelia. *Biochem Cell Biol.* 2014;92(6):467-480.
38. Karbach U, Rummel W. Trans- and paracellular calcium transport across the colonic mucosa after short- and long-term treatment with 1,25-dihydroxyvitamin D₃. *Eur J Clin Invest.* 1986;16(5):347-351.
39. Karbach U, Rummel W. Calcium transport across the colon ascendens and the influence of 1,25-dihydroxyvitamin D₃ and dexamethasone. *Eur J Clin Invest.* 1987;17(4):368-374.
40. Wongdee K, Rodrat M, Teerapornpuntakit J, Krishnamra N, Charoenphandhu N. Factors inhibiting intestinal calcium absorption: hormones and luminal factors that prevent excessive calcium uptake. *J Physiol Sci.* 2019;69(5):683-696.
41. Gutekunst L. An update on phosphate binders: a Dietitian's perspective. *J Ren Nutr.* 2016;26:209-218.
42. Fuqua BK, Vulpe CD, Anderson GJ. Intestinal iron absorption. *J Trace Elem Med Biol.* 2012;26(2-3):115-119.
43. Collins JF, Franck CA, Kowdley KV, Ghishan FK. Identification of differentially expressed genes in response to dietary iron deprivation in rat duodenum. *Am J Physiol - Gastrointest Liver Physiol.* 2005;288(5):G964-G971.
44. Collins JF. Gene chip analyses reveal differential genetic responses to iron deficiency in rat duodenum and jejunum. *Biol Res.* 2006;39(1):25-37.
45. Fox J, Green DT. Direct effects of calcium channel blockers on duodenal calcium transport in vivo. *Eur J Pharmacol.* 1986;129(1-2):159-164.
46. Forster IC, Virkki L, Bossi E, Murer H, Biber J. Electrogenic kinetics of a mammalian intestinal type IIb Na⁺/Pi cotransporter. *J Membr Biol.* 2006;212(3):177-190.
47. Marks J, Debnam ES, Unwin RJ. Phosphate homeostasis and the renal-gastrointestinal axis. *Am J Physiol Ren Physiol.* 2010;299:285-296.
48. Günzel D, Yu ASL. Claudins and the modulation of tight junction permeability. *Physiol Rev.* 2013;93(2):525-569.
49. Colegio OR, Van Itallie C, Rahner C, Anderson JM. Claudin extracellular domains determine paracellular charge selectivity and resistance but not tight junction fibril architecture. *Am J Physiol - Cell Physiol.* 2003;284(6):C1346-C1354.
50. Yu ASL, Cheng MH, Angelow S, et al. Molecular basis for cation selectivity in claudin-2-based paracellular pores: Identification of an electrostatic interaction site. *J Gen Physiol.* 2009;133(1):111-127.
51. Curry JN, Saurette M, Askari M, et al. Claudin-2 deficiency associates with hypercalciuria in mice and human kidney stone disease. *J Clin Invest.* 2020;130(4):1948-1960.
52. Kutuzova GD, DeLuca HF. Gene expression profiles in rat intestine identify pathways for 1,25-dihydroxyvitamin D₃ stimulated calcium absorption and clarify its immunomodulatory properties. *Arch Biochem Biophys.* 2004;432(2):152-166.
53. Tandy S, Williams M, Leggett A, et al. Nramp2 expression is associated with pH-dependent iron uptake across the apical membrane of human intestinal Caco-2 cells. *J Biol Chem.* 2000;275(2):1023-1029.
54. Brun LR, Brance ML, Rigalli A. Luminal calcium concentration controls intestinal calcium absorption by modification of intestinal alkaline phosphatase activity. *Br J Nutr.* 2012;108(2):229-233.
55. Marks J, Churchill LJ, Debnam ES, Unwin RJ. Matrix extracellular phosphoglycoprotein inhibits phosphate transport. *J Am Soc Nephrol.* 2008;19(12):2313-2320.
56. Bonsnes RW, Taussky HH. On colorimetric determination of creatinine by the Jaffe reaction. *J Biol Chem.* 1945;158(3):581-591.
57. Bradford MM. A rapid and sensitive method for the quantitation of microgram quantities of protein utilizing the principle of protein-dye binding. *Anal Biochem.* 1976;72(1-2):248-254.

58. Forstner GG, Tanaka K, Isselbacher KJ. Lipid composition of the isolated rat intestinal microvillus membrane. *Biochem J.* 1968;109(1):51-59.

SUPPORTING INFORMATION

Additional Supporting Information may be found online in the Supporting Information section.

How to cite this article: Asowata EO, Olusanya O, Abaakil K, et al. Diet-induced iron deficiency in rats impacts small intestinal calcium and phosphate absorption. *Acta Physiol.* 2021;232:e13650. <https://doi.org/10.1111/apha.13650>